

Carbon coating of fused silica ampoules

Mark J. Harrison, Adam P. Graebner, Walter J. McNeil, Douglas S. McGregor*

S.M.A.R.T. Laboratory, Department of Mechanical and Nuclear Engineering, Kansas State University, Manhattan, KS 66506, USA

Received 22 September 2005; received in revised form 5 January 2006; accepted 10 January 2006

Available online 20 March 2006

Communicated by T. Hibiya

Abstract

A reliable method for depositing a layer of carbon on the inner walls of a fused silica ampoule is described and characterized. Carbon deposition rates were found to be $0.33\ \mu\text{m}/\text{h}$ at mid-length and range from 0.26 to $0.55\ \mu\text{m}/\text{h}$ at the ends of a 150 mm long ampoule. Deposition rate was found to vary along the length of the ampoule, but not along the radial perimeter.

© 2006 Elsevier B.V. All rights reserved.

Keywords: A1. Ampoule preparation; A1. Carbon coating; A2. Growth from melt; B1. Quartz

1. Introduction

Fused synthetic silica (quartz) is often used in the construction of the crucible or ampoule in crystal growth or materials purification applications for a number of reasons. Quartz is readily available in very pure form while possessing the ability to withstand high temperatures and high thermal gradients. The material also maintains good mechanical strength at elevated temperatures. However, for all of the beneficial properties of quartz, devitrification and other deleterious effects occur in the presence of some materials.

Certain processes benefit from a thin coating of carbon deposited on the quartz sidewalls as the carbon can act as a scavenger of oxygen (O_2) and water (H_2O) impurities and as a protective buffer between the material of concern and the quartz [1]. In the case of Bridgman growth of cadmium telluride (CdTe) or cadmium zinc telluride (CdZnTe), the ingot tends to adhere to the sidewalls of the quartz vessel in which it is grown. Presumably, cadmium oxide (CdO) reacts with the silicon in the sidewall to form cadmium metasilicate (CdSiO_3) [1]. However, at elevated temperatures, carbon reacts easily with O_2 and H_2O to form carbon dioxide (CO_2) and carbon monoxide (CO), thus tying up otherwise free O_2 molecules. Without the presence of free

oxygen, the reaction between CdO and quartz is much less severe since CdO does not initially form. Therefore, the inclusion of carbon within the ampoule serves two purposes. The first purpose is to getter any O_2 or H_2O . Second, the carbon layer physically prevents CdO from contacting the inner ampoule walls. Similar benefits are reported for the growth of copper indium selenide (CuInSe_2) [2].

The carbon coating process and its effects on crystal growth are mentioned several times in the literature [1–9]. However, a definitive procedure for obtaining uniform, adherent coatings of carbon is not present. This work describes a reliable, reproducible carbon coating technique and presents data regarding the thickness of coatings at various locations along the ampoule.

2. Experimental procedure

The process described here requires four basic steps: ampoule cleaning, ampoule annealing, carbon deposition, and film annealing. The cleaning and annealing procedures were found to greatly impact carbon film quality and are therefore included. Carbon deposition is the process of cracking hydrocarbon molecules to produce an amorphous carbon layer. The deposited carbon film must be then heated to sufficiently high temperatures to densify the layer into a glass-like form of lower porosity. Each of these four steps for obtaining a uniform, well-adhered carbon film on

*Corresponding author. Tel.: +1 785 532 5284; fax: +1 785 532 7057.
E-mail address: mcmgregor@ksu.edu (D.S. McGregor).

the inner walls of a quartz ampoule is explained in detail in the following sections.

A total of four quartz ampoules were used in studying this process. All ampoules were built by Technical Glass Products, Inc. to specified dimensions using high-purity quartz stock. A cross-sectional view of the ampoule design is given in Fig. 1 with the specified dimensions. The rounded end nearest point D is referred to as the bottom, because of the ampoule's orientation during vertical Bridgman crystal growth. Each ampoule had a main chamber constructed of 25×28 mm quartz tube with a short support rod at the bottom and a $\frac{3}{8}$ in inlet tube on the opposite end. While the ampoules used here had a hemispherical bottom end, the ampoules used for crystal growth purposes usually utilize conical ends to aid in grain seeding. No differences in carbon coating of either design have been noted. The interior of the ampoule was not roughened, unlike in literature elsewhere [9].

2.1. Cleaning

Each ampoule was, in turn, cleaned within a Class 1000 cleanroom using a series of etches and rinses designed to minimize impurities within the ampoule. The steps for cleaning are listed in Table 1. All glassware used to prepare the solutions was cleaned in the same manner as the ampoule prior to use. Upon completion of the cleaning steps, the inlet tube was sealed using Parafilm and the outer surface of the ampoule wiped with isopropanol prior to being removed from the cleanroom. Any ampoule handling

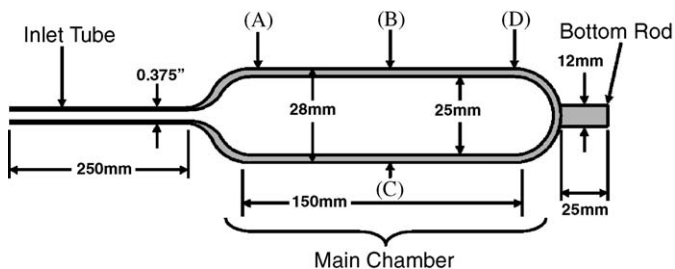


Fig. 1. Cross-sectional view of quartz ampoule. Points A–D denote positions which were measured for carbon thickness.

Table 1

Step	Description
1	Rinsed 6 times with deionized water (DI H ₂ O)
2	Etched for 15 min with 1:1:1 H ₂ SO ₄ :H ₂ O ₂ :DI H ₂ O solution at room temperature (RT)
3	Rinsed 6 times with DI H ₂ O
4	Etched for 2.5 h with potassium dichromate acid at RT
5	Rinsed 6 times with DI H ₂ O
6	Etched for 4 h with 5% HF/DI H ₂ O solution at RT
7	Rinsed 6 times with DI H ₂ O
8	Rinsed 4 times with Certified ACS (American Chemical Society) grade isopropanol

after this point was done by touching the bottom rod or inlet stem with nitrile gloves, never the outer walls of the main chamber.

2.2. Ampoule annealing

Next, each ampoule was inserted into a three-zone horizontal clamshell furnace for processing immediately after being cleaned. The main chamber of each ampoule was placed within the center zone (Zone 2) of the furnace as depicted in Fig. 2. The inlet tube extended out of one end of the furnace. To ensure uniform heating, the ampoule was centered within the furnace by placing alumina insulation rings around the support rod and the inlet tube on either side of the main chamber. Two more alumina rings were also placed around the inlet tube at equal intervals along its length to help reduce sag at the high processing temperatures.

A series of stainless steel fittings were next attached to the inlet tube. A larger diagram of the arrangement is shown in Fig. 3. This set of fittings played several important roles. Moving to the left from seal 1, the first component was an “Inlet Ball Valve” of sufficient diameter to allow a small 2×3 mm quartz tube to pass through when the valve was open. Next, a tee allowed an exhaust for flow gases. Finally, seal 2 sealed around the 2×3 mm tube. The 2×3 mm quartz tube was used to insert gases into the ampoule and was approximately the same length as the ampoule and fittings combined. This “gas insertion tube” was inserted into the ampoule leaving 25 mm of clearance between the bottom end of the ampoule and the exit point of the gas insertion tube. A gas line was finally sealed onto the gas insertion tube to the left of seal 2.

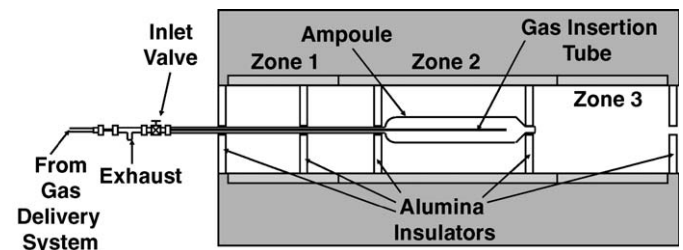


Fig. 2. Cross-sectional view of ampoule within the three zone tube furnace.

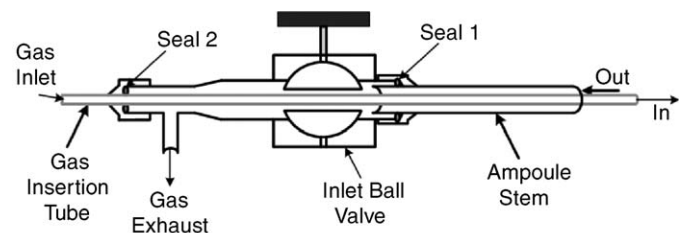


Fig. 3. Cross-sectional view of the gas insertion tube sealing apparatus.

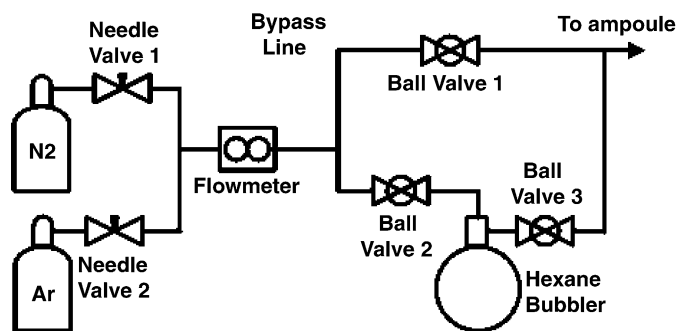


Fig. 4. Piping and instrumentation diagram of the gas flow apparatus.

Once mounted, the ampoule was ready to be annealed. To begin, ultra-high-purity (UHP) argon was used to purge the ampoule of any residual isopropanol or water using a flow rate of approximately 100 mL/min. During the purging, the furnace was ramped to 1160 °C at a rate of 3 °C/min. Fig. 4 depicts the arrangement of valving and instrumentation used to achieve the gas flows and flow rates described. When the furnace reached 200 °C, the argon flow rate was reduced to 15 mL/min. Once the furnace reached 1160 °C, the temperature and gas flow rate were held constant for at least 8 h to anneal the quartz.

2.3. Carbon deposition

Upon completion of the annealing step, the furnace temperature was lowered to the carbon deposition temperature of 700 °C at a rate of 1 °C/min to avoid introducing stress back into the ampoule as it cooled. When 700 °C had been reached, the argon flow was switched to an UHP nitrogen (N₂) gas flow of 15 mL/min. For 1 h, temperature and N₂ gas flow were held constant to purge the ampoule of argon and ensure the temperature field was near or at an equilibrium of 700 °C.

Carbon deposition was started by diverting the N₂ gas flow from bypassing the hexane bubbler to flowing through the bubbler to begin carrying hexane into the heated ampoule. N₂ flow was held constant at 15 mL/min for the duration of the deposition period. The duration of this deposition step was varied for the purposes of this thickness study and was set at 1/2, 1, 2, and 3 h long for the four ampoules. Spectrophotometric hexane was chosen as the hydrocarbon for carbon deposition as it is readily available in high-purity form and contains no oxygen at the molecular level. However, other hydrocarbons such as acetone, propane, isopropanol, and methanol have been used with success by others in different carbon coating processes [10].

2.4. Film annealing

At the conclusion of the carbon deposition, the N₂ gas flow was again switched to bypass the bubbler for 1 h to purge the lines and ampoule of residual hexane. While N₂

continued to flow at 15 mL/min to maintain a positive pressure on the system, seal 2 was detached from the outlet tee. The gas insertion tube was then slowly removed. As soon as the end of the gas insertion tube cleared the inlet valve, the inlet ball valve was closed. N₂ flow was stopped and the gas insertion tube was fully removed from the fittings. Next, the outlet tee was disconnected from the inlet valve and removed from the system. A mechanical roughing pump was then connected to the inlet valve. The vacuum pump was switched on and the foreline was pumped down to less than 150 mTorr. Over a period of several minutes, the inlet valve was slowly opened to evacuate the ampoule. The system pressure stabilized at 150 mTorr after several minutes of pumping. The furnace was next ramped from the deposition temperature of 700 °C to the film annealing temperature of 1150 °C at 3 °C/min. The ampoule was held at 1150 °C under a vacuum of 150 mTorr for 2 h to anneal the carbon film.

Once annealing was completed, the furnace was ramped down to room temperature at 1 °C/min. When the furnace had reached a temperature of less than 100 °C, the inlet valve was closed again and the vacuum pump detached. Argon flow was again introduced to the system to backfill the ampoule to atmospheric pressure.

3. Results

The carbon-coated ampoules appeared as shown in Fig. 5 when removed from the furnace. Samples located at points A–D were cut from each ampoule using a diamond-wire saw. The depth of carbon on each sample was measured using a Hitachi S-3500 scanning electron microscope (SEM). A representative photograph of the depth measurements is shown in Fig. 6. Energy dispersive X-ray analysis confirmed the location of the carbon on the quartz (SiO₂) substrate.

For the deposition times of 1/2, 1, 2 and 3 h used, the resulting carbon depths are presented in Figs. 7–9. Carbon depth did not vary significantly between points B and C for any deposition time as seen in Fig. 8. Carbon depth is plotted against location for all deposition lengths in Fig. 10.

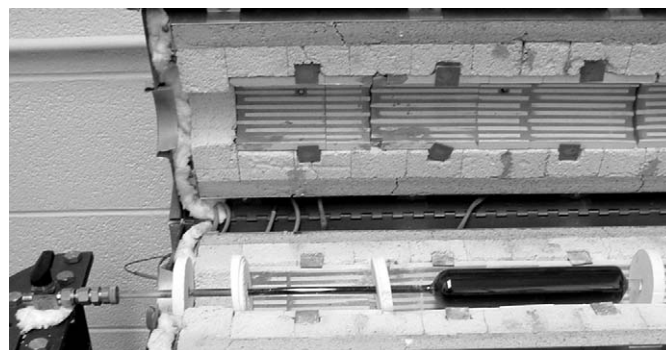


Fig. 5. Carbon-coated ampoule mounted in furnace.

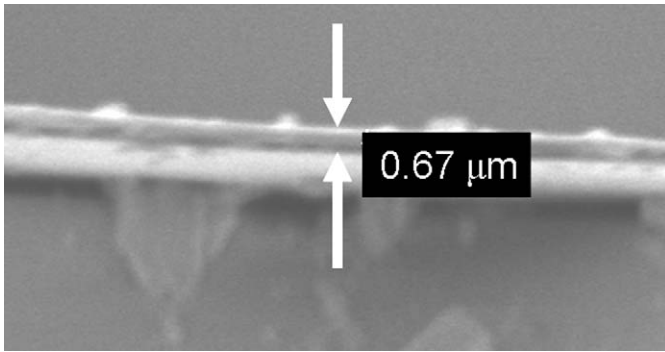


Fig. 6. SEM photo of a carbon film on a quartz ampoule wall.

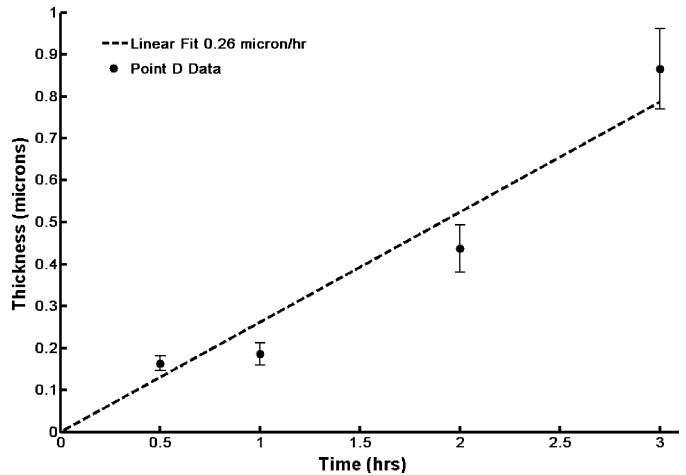


Fig. 9. Measured depths at Point D. Solid line represents the theoretical line of best fit.

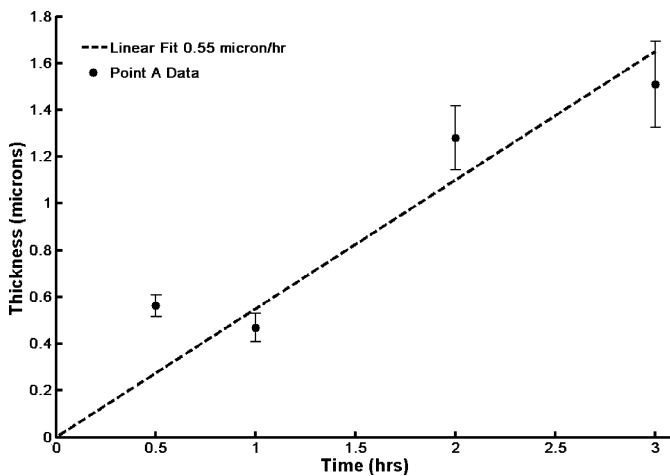


Fig. 7. Measured depths at Point A. Solid line represents the theoretical line of best fit.

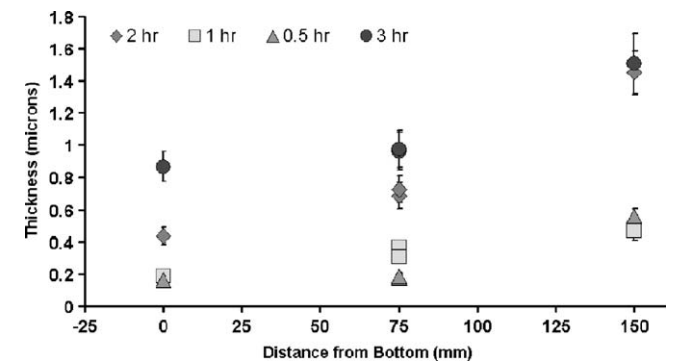


Fig. 10. Carbon depth as a function of axial location.

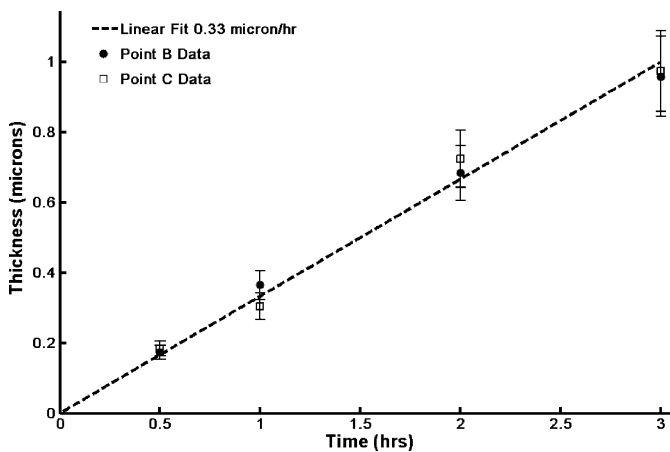


Fig. 8. Measured depths at Points B and C. Solid line represents the theoretical line of best fit.

4. Conclusion

Carbon depth was found to vary considerably in the axial direction, but very little in the radial direction. As is evident from the data at points B and C in Fig. 8, ampoule

orientation made little difference upon the deposition rate where both points had deposition rates near $0.33 \mu\text{m/h}$ when the data are regressed to a straight line passing through the origin. However, comparing data taken from points A and D in Figs. 7 and 9, it is seen that deposition rate varies considerably, across the range $0.26\text{--}0.55 \mu\text{m/h}$.

Fig. 10 clearly illustrates how deposition rate varied with axial location. Note that all sets of data show an upward trend moving from point A to point D or, rather, from the ampoule bottom to the inlet tube.

During the course of characterizing the carbon deposition process, the film was noted to flake off of the ampoule side walls for “long” deposition times. The ampoule used for the characterization study, Fig. 2, tended to shed the carbon film for depositions exceeding 6 h. Once the film had separated from the sidewalls, deposition restarted at that location. Evidence, therefore, suggests that an upper limit to carbon thickness exists for the described process.

While an upper limit may exist for the carbon thickness, carbon films of approximately $1.1 \mu\text{m}$ thick have proven to be sufficient for preventing ingot adherence to ampoules in CdZnTe growth. The process previously described is a reliable and predictable method of producing carbon films of magnitudes on the order of $1.5 \mu\text{m}$.

Acknowledgments

The authors would like to gratefully acknowledge Dr. Krishna Mandel, Dr. F. Patrick Doty, and Dr. Muren Chu for relating their experiences and providing invaluable assistance in creating the process for carbon deposition. This work was supported in part by the Department of Energy under NEER Grant #031D14498.

References

- [1] E. Raiskin, J.F. Butler, IEEE Trans. Nucl. Sci. NS-35 (1987) 81.
- [2] L.S. Yip, I. Shih, C.H. Champness, J. Crystal Growth 129 (1993) 102.
- [3] R. Triboulet, Y. Marfaing, J. Electrochem. Soc. 120 (1973) 1260.
- [4] C. Martinez-Tomas, V. Munoz, R. Triboulet, J. Crystal Growth 197 (1999) 435.
- [5] C. Martinez-Tomas, V. Munoz, J. Crystal Growth 222 (2001) 435.
- [6] M. Bruder, H.J. Schwarz, R. Schmitt, H. Maier, M.O. Moeller, J. Crystal Growth 101 (1990) 266.
- [7] H.L. Glass, A.J. Socha, C.L. Parfeniuk, D.W. Bakken, J. Crystal Growth 184/185 (1998) 1035.
- [8] W. Sang, Y. Qian, W. Shi, L. Wang, J. Yang, D. Liu, J. Crystal Growth 214/215 (2000) 30.
- [9] H. Qingrun, G. Ju, Rare Metals 16 (1997) 156.
- [10] F. Patrick Doty, Sandia National Laboratory, Personal communication, 2004.